

ADVANCED COMPUTATIONAL TECHNIQUES FOR THE DESIGN OF DEFORMATION PROCESSES

AFOSR CONTRACT NO. F49620-00-1-0373

Nicholas Zabaras

Materials Process Design and Control Laboratory,
Sibley School of Mechanical and Aerospace Engineering, 188 Frank H. T. Rhodes Hall
Cornell University, Ithaca, NY 14853-3801
URL: <http://www.mae.cornell.edu/zabaras/>

Objectives

The objective of this work is to develop a continuum sensitivity finite element analysis for the robust design of multi-stage metal forming processes in aircraft manufacturing. The computational forming design simulator being developed is applied to industrial forming design and provides the means to select the sequence of deformation processes, design the dies and preforms for each process stage as well as the process conditions such that a product is obtained with desired shape and microstructure and with the minimal material utilization and overall cost. This virtual process laboratory will assist the aircraft manufacturing industry in reducing time for process and product development, in trimming the cost of an extensive experimental process development effort and in developing processes for tailored material properties.

1 Status of Effort

Substantial progress was accomplished towards the project objectives during the last year of this AFOSR award. Particular contributions are summarized below:

- Development of phenomenology based design simulator for the control of microstructure in the presence of dynamic recrystallization and grain growth mechanisms during deformation processes [1].
- Extending existing design simulator towards 3D analysis – including the development of continuum sensitivity analysis for contact problems [2].
- A computational framework for multi-length scale design was developed for the control of properties that are inherently dependent on texture – Reduced order modeling (proper orthogonal decomposition) schemes were developed for computationally efficient design schemes, based on viscoplastic polycrystal models [3, 4].
- Finally, work is in progress towards the development of a design simulator based on thermoelastic-viscoplastic constitutive modeling of polycrystalline materials [5].

The developed forming design simulator can at present address a variety of design problems for geometrically complex two-dimensional, axisymmetric and three-dimensional multi-stage deformation processes. A total and updated Lagrangian framework is used that allows accurate data transfer operations during remeshing in both the direct and sensitivity analyses [6]. Multi-objective design optimization is considered and various constraints can be imposed on the process conditions or the design variables.

1.1 Process design for the control of microstructure [1]

The idea of control of mechanical properties in materials through designer processing techniques was promoted through this effort. Microstructure evolution through dynamic recrystallization is accurately modeled for the large thermo-mechanical deformation of hyperelastic thermo-viscoplastic materials. Innovative solution strategy and computational algorithms were developed for the solution of the direct and sensitivity deformation problems. The description relies on microstructure based scalar state variables [1]. The total deformation gradient is decomposed into thermal, plastic and elastic parts as $F = F^e F^p F^\theta$. The constitutive equations are developed on the intermediate unstressed configuration [10]. Microstructure related length scales are now introduced into the constitutive framework to model the dependence of the material behavior on its recrystallized state. We describe the microstructure through internal state variables linked to the grain size as followed in [6]. The evolution of the

equivalent plastic strain is specified as, $\dot{\epsilon}^p = f(\sigma, s, \theta, \frac{L_0}{L})$ where σ is the equivalent stress, s is

the state variable denoting deformation resistance, θ is the absolute temperature and L denotes the mean grain size. The evolution of the isotropic scalar resistance S is assumed to take the form,

$\dot{s} = g(\sigma, s, \theta, \frac{L_0}{L}) = h(\sigma, s, \theta, \frac{L_0}{L}) - \dot{r}(\sigma, s, \theta, \frac{L_0}{L})$, where $h(\sigma, s, \theta, \frac{L_0}{L})$ can be interpreted as

the rate at which dislocation density changes during deformation and $\dot{r}(\sigma, s, \theta, \frac{L_0}{L})$ is the dynamic recovery function. Further, the evolution of the average grain size during and immediately after primary recrystallization (during dynamic recrystallization) is considered to be governed by the

following equation, $\dot{L} = \dot{L}_{ref} + \dot{L}_{grow}$, where \dot{L}_{ref} is the rate of overall grain refinement taking place during primary recrystallization and \dot{L}_{grow} represents the kinetics of the grain growth process during secondary recrystallization. A mathematically rigorous extension of the CSM (continuum sensitivity method) to the material model described above was introduced [1]. Full design-differentiation of all material constitutive equations were performed for both shape and process parameter sensitivity analysis. Fig. 1 highlights a two stage process design problem, where the design parameter is the preforming die shape. The material was chosen to be 0.2 % C steel initially at 1213K.

primary recrystallization and \dot{L}_{grow} represents the kinetics of the grain growth process during secondary recrystallization. A mathematically rigorous extension of the CSM (continuum sensitivity method) to the material model described above was introduced [1]. Full design-differentiation of all material constitutive equations were performed for both shape and process parameter sensitivity analysis. Fig. 1 highlights a two stage process design problem, where the design parameter is the preforming die shape. The material was chosen to be 0.2 % C steel initially at 1213K.

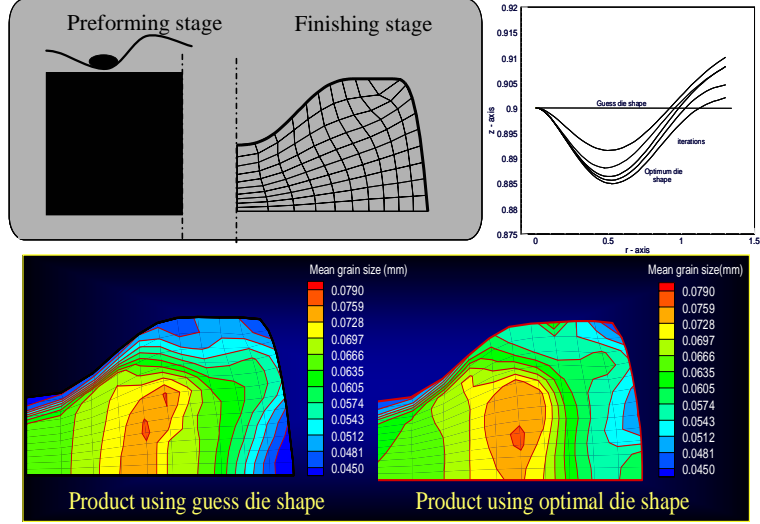


Fig. 1 Two stage forging process design – Design the preforming die in a 2 stage process with a fixed finishing die so as to minimize the variation in the grain sizes in the finished product [1].

1.2 Sensitivity contact problem [2]

The sensitivity contact problem involves computing the sensitivities of the contact traction vector. It can be written as

$$\overset{o}{\lambda} = \overset{o}{\lambda}_N \overset{o}{\mathbf{v}}(\bar{\mathbf{y}}) + \overset{o}{\lambda}_{T_1} \overset{o}{\mathbf{v}}(\bar{\mathbf{y}}) - \overset{o}{\lambda}_{T_1} \overset{o}{\boldsymbol{\tau}}^1(\bar{\mathbf{y}}) - \overset{o}{\lambda}_{T_1} \overset{o}{\boldsymbol{\tau}}^1(\bar{\mathbf{y}}) - \overset{o}{\lambda}_{T_2} \overset{o}{\boldsymbol{\tau}}^2 - \overset{o}{\lambda}_{T_2} \overset{o}{\boldsymbol{\tau}}^2(\bar{\mathbf{y}}) \quad (1)$$

where $\overset{o}{\boldsymbol{\tau}}^1(\bar{\mathbf{y}})$ and $\overset{o}{\boldsymbol{\tau}}^2(\bar{\mathbf{y}})$ are the sensitivities of the contravariant components of the tangent vectors. To allow for the computation of the design derivatives, certain regularization assumptions are introduced:

- A particle that lies in the admissible (or inadmissible) region for the direct problem also lies in the admissible (or inadmissible) region for the sensitivity problem.
- A point that is in a state of slip (or stick) in the direct problem is also in the same state in the sensitivity problem.

As a result of the above assumptions, Eq. (1) gives a complete description of the sensitivity contact

problem. The quantities $\overset{o}{\lambda}_N, \overset{o}{\lambda}_{T_1}, \overset{o}{\lambda}_{T_2}, \overset{o}{\mathbf{v}}(\bar{\mathbf{y}}), \overset{o}{\boldsymbol{\tau}}^1(\bar{\mathbf{y}})$ and $\overset{o}{\boldsymbol{\tau}}^2(\bar{\mathbf{y}})$ depend on the sensitivities of the

closest point projection $[\overset{o}{\xi}^1, \overset{o}{\xi}^2]$ which in turn depend on the sensitivity of the displacements $\overset{o}{\mathbf{x}}$. The sensitivity of the covariant form of the tangent vector takes the form,

$$[\overset{o}{\boldsymbol{\tau}}_\alpha] = [\overset{o}{\boldsymbol{\tau}}_\alpha(\bar{\mathbf{y}})] = [\overset{o}{\mathbf{y}}_{,\xi^\alpha}] = \overset{o}{\mathbf{y}}_{,\xi^\alpha} + \bar{\mathbf{y}}_{,\xi^\alpha \xi^\alpha} \overset{o}{\xi}^\alpha + \bar{\mathbf{y}}_{,\xi^\alpha \xi^\beta} \overset{o}{\xi}^\beta \quad (\text{no sum}).$$

The contravariant form can be

obtained from the above by the following expression $[\overline{\boldsymbol{\tau}}^\alpha] = m^{\alpha\beta} [\overline{\boldsymbol{\tau}}_\beta] + m^{\alpha\beta} \boldsymbol{\tau}_\beta$, where $m^{\alpha\beta}$ denotes the sensitivity of the metric tensor $m^{\alpha\beta}$ in the given coordinate system. The sensitivity of the normal vector can be written as,

$$\overline{[\mathbf{v}]} = \overline{[\mathbf{v}(\overline{\mathbf{y}})]} = \frac{\overline{\boldsymbol{\tau}_1 \times \boldsymbol{\tau}_2}}{\|\overline{\boldsymbol{\tau}_1 \times \boldsymbol{\tau}_2}\|} = \frac{[\overline{\boldsymbol{\tau}_1}] \times \boldsymbol{\tau}_2}{\|\boldsymbol{\tau}_1 \times \boldsymbol{\tau}_2\|} + \frac{\boldsymbol{\tau}_1 \times [\overline{\boldsymbol{\tau}_2}]}{\|\boldsymbol{\tau}_1 \times \boldsymbol{\tau}_2\|} + \boldsymbol{\tau}_1 \times \boldsymbol{\tau}_2 \left(\frac{1}{\|\boldsymbol{\tau}_1 \times \boldsymbol{\tau}_2\|} \right)$$

The remaining quantities $\overset{\circ}{\lambda}_N$, $\overset{\circ}{\lambda}_{T_1}$ and $\overset{\circ}{\lambda}_{T_2}$ are computed by considering the constraints that are used for evaluating the quantities λ_N , λ_{T_1} and λ_{T_2} in the direct deformation problem. Similar to the direct problem, $\overset{\circ}{\lambda}_N$, $\overset{\circ}{\lambda}_{T_1}$ and $\overset{\circ}{\lambda}_{T_2}$ can be thought of as the Lagrange multipliers for the sensitivity problem. To enforce the normal contact constraints in the sensitivity problem the following penalization is used: $\overset{\circ}{\lambda}_N = \overset{\circ}{\lambda}_{N_n} + \varepsilon_N \overset{\circ}{g}(\mathbf{x}_{n+1})$, where $\overset{\circ}{\lambda}_{N_n}$ is the normal traction sensitivity calculated in the previous time step and $\overset{\circ}{g}(\mathbf{x}_{n+1})$ is the sensitivity of the gap function. To enforce the tangential contact constraints

for sticking the following penalization is used: $m_{\alpha\beta} \overset{\circ}{\xi}^\beta = \frac{1}{\varepsilon_T} \overset{\circ}{\lambda}_{T_\alpha}$, which on integration leads to

$$\overset{\circ}{\lambda}_{T_\alpha} = \overset{\circ}{\lambda}_{T_{n\alpha}} + \varepsilon_T m_{\alpha\beta} (\overset{\circ}{\xi}^\beta - \overset{\circ}{\xi}_n^\beta) \quad \alpha, \beta = 1, 2; \text{ where } \overset{\circ}{\lambda}_{T_{n\alpha}} \text{ and } \overset{\circ}{\xi}_n^\beta \text{ are known from the previous time}$$

step. For sliding contact $\overset{\circ}{\lambda}_{T_\alpha}$ is calculated from the expression $\overset{\circ}{\lambda}_{T_\alpha} = \left(\frac{\mu \lambda_N}{\|\boldsymbol{\lambda}_T\|} \right) \overset{\circ}{\lambda}_{T_\alpha}^{trial} \quad \alpha = 1, 2$. An

important point to be noted here is the presence of the term $\overset{\circ}{\lambda}_{T_\alpha}^{trial}$, which is the trial tangent traction calculated in the radial return mapping scheme in the direct problem. i.e. the sensitivity of the traction term depends on the trial traction and not just the current traction value. After some rigorous mathematics, the above contact traction sensitivities can be expressed concisely as follows: $\overset{\circ}{\lambda} = g \overset{\circ}{\zeta}_1 + \overset{\circ}{\xi}^1 \overset{\circ}{\zeta}_2 + \overset{\circ}{\xi}^2 \overset{\circ}{\zeta}_3 + \overset{\circ}{\zeta}_4$. The linear relationship between $\overset{\circ}{\xi}^\alpha$ and $\overset{\circ}{\mathbf{x}}$ can be developed by

considering the sensitivity of the expression $(\overline{\mathbf{y}} - \mathbf{x}) \cdot \boldsymbol{\tau}_\alpha(\overline{\mathbf{y}}) = 0$. The relationship between $\overset{\circ}{g}$ and $\overset{\circ}{\mathbf{x}}$ can be developed by design differentiation of the gap function. To avoid augmentations to the Lagrange multipliers in the sensitivity problem and using the fact that the sensitivity problem is linear (thus no convergence problems), we compute the sensitivities of the contact tractions in one step by using oversize penalties. The three-dimensional sensitivity analysis highlighted in this section is novel, mathematically rigorous and capable of providing very accurate sensitivities.

1.3 Preform design for open die forging of a cylinder [2]

In this example the objective is to design the optimum preform shape of variant volume for flat die upsetting of a cylinder so as to minimize barreling in the final product. The process is assumed to be isothermal. The initial height and the radius of the preform are taken as 3.0 mm and 1.0 mm, respectively. The forging velocity is fixed at 0.01mm/s. The friction coefficient is taken as 0.4. The final desired height and radius are 2.0 mm and 1.464 mm, respectively. The stroke is fixed at 1.0 mm, which corresponds to a total deformation of 33%. Using

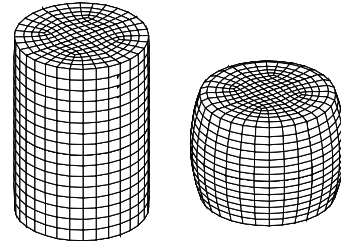


Fig. 2 Initial preform and final forged product for the cylinder upsetting problem (section 1.3) [2]

symmetry conditions only one-eighth of the domain is used for computation. The final forged product obtained using the initial preform shape is plotted in Fig. 2. The major axes and minor axes of the ellipse are each modeled using degree 6 Bezier curves. Using the restriction that $x'(\alpha) = 0$ and $y'(\alpha) = 0$, the free surface can be represented using 12 design variables β_i ($i = 1..12$):

$$x(\alpha) = a \cos \theta \quad y(\alpha) = b \sin \theta$$

$$a(\alpha) = \sum_{i=1}^6 \beta_i \phi_i(\alpha) \quad b(\alpha) = \sum_{i=1}^6 \beta_{i+6} \phi_i(\alpha)$$

$$\phi_1 = (1.0 - \alpha)^5 (1.0 + 5.0\alpha) \quad \phi_2 = 15.0(1.0 - \alpha)^4 \alpha^2$$

$$\phi_3 = 20.0(1.0 - \alpha)^3 \alpha^3 \quad \phi_4 = 15.0(1.0 - \alpha)^2 \alpha^4$$

$$\phi_5 = 6.0(1.0 - \alpha)^2 \alpha^5 \quad \phi_6 = \alpha^6$$

$$z = \alpha / H$$

where $a(\alpha)$ and $b(\alpha)$ denote the major and minor axes of the resulting elliptical cross section and H denotes the height of the cylinder. Thus the design vector can be defined as $\beta = \{\beta_1, \beta_2, \beta_3, \beta_4, \beta_5, \beta_6, \beta_7, \beta_8, \beta_9, \beta_{10}, \beta_{11}, \beta_{12}\}^T$. For the shape optimization problem the objective function is defined as

$$\min_{\beta} f(\beta) = \frac{1}{2N} \sum_{i=1}^N (\sqrt{x_i(\beta)^2 + y_i(\beta)^2} - r_0)^2$$

where N denotes the number of points along the curved boundary and r_0 is the desired radius of the final forged product. The objective function is minimized using a gradient optimization framework where the gradient of the objective function is calculated from the sensitivities computed in the sensitivity problem. The optimal preform and the final forged product are plotted in Fig. 3.

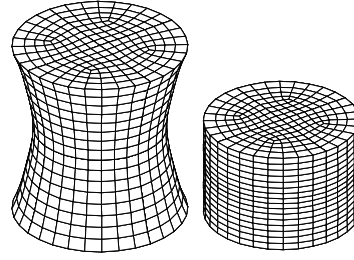


Fig. 3 Preform and final forged product for the cylinder upsetting problem (section 1.3) [2].

1.4 Multi-length scale design: Design for texture dependent properties [3, 4]

A novel reduced-order modeling approach to represent crystallographic texture in polycrystals has been developed. Most process design applications are quite sensitive to the anisotropy of the crystalline materials. The anisotropy is primarily due to the crystallographic texture, which can be defined as a preferred orientation of the crystals in a particular direction. Recent work in the field of texture analysis and modeling has concentrated on representation of texture evolution by an orientation distribution function (ODF). The ODF represents the probability density of finding a crystal orientation within the three-dimensional orientation space. Texture evolution is described over the orientation space through the solution of the ODF conservation equation. An approach, different from the common use of Fourier series or generalized harmonics,

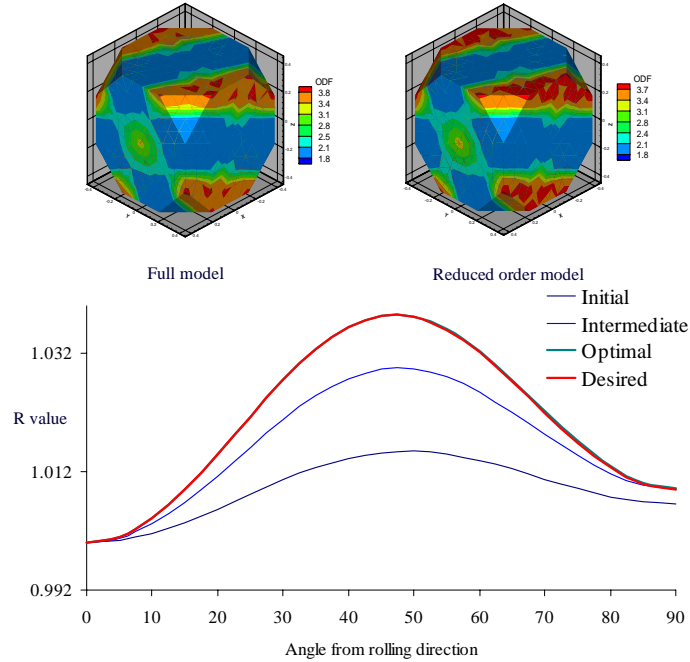


Fig. 4 Control of the R-parameter through deformation process [4]. The desired R-parameter is obtained by designing for the velocity gradient. Two schemes, i.e. the full model and the reduced model were used for this problem. Shown are the optimum ODF distributions for each scheme as well as the distribution of the R-parameter at different stages of the optimization problem (using the reduced modeling scheme).

has been utilized where a finite element representation of the ODF using angle-axis parameterization was proposed. In this scheme, the ODF is represented over the finite element Rodrigues space using polynomial shape functions defined locally over each element. These shape functions provide local support and are suitable for representing sharp textures in contrast to the series expansion schemes which provide global support and are thus not very suitable for sharp textures. An effective multiscale model calls for an accurate representation of the microstructural features. A full description of the microstructure would involve a large number of degrees of freedom and require significant computing resources and time. Microstructure model reduction is thus not only useful but possibly the only means to eventually allow for an effective process design and control that leads to desired properties of polycrystals. This method involves generation of a reduced orthogonal basis for representing polycrystal texture in Rodrigues space [3]. The reduced basis is generated from the textures obtained from different deformation modes (shear, tension, etc.) using proper orthogonal decomposition and the method of snapshots. This model reduction can account for all essential information needed to describe the microstructure and leads to tremendous savings in computational time. Based on the above method a multiscale model for microstructure evolution during deformation has been proposed driven by the macroscale velocity gradient. A continuum sensitivity-based gradient optimization framework is introduced in the above model for control of microstructure-sensitive material properties. Emphasis is given towards design problems that demonstrate the effectiveness of the above method for optimal control of texture-dependent material properties during deformation such as the magnetic hysteresis losses, the yield stress and the Lankford parameter R [3, 4]. The evolution of the ODF (orientation distribution function), represented by $A(\mathbf{r}, t)$ with \mathbf{r} defining the orientation (neo-Eulerian parametrization), is given in [3] as $\frac{\partial A}{\partial t} + \nabla A \cdot \mathbf{v} + A \nabla \cdot \mathbf{v} = 0$, where $\mathbf{v}(\mathbf{r}, t)$ is the Eulerian reorientation velocity. [3, 4] highlight the solution scheme as well as validating the scheme and summarize interesting results. The ODF in a reduced model is approximated as $A(\mathbf{r}, t) = \sum_{j=1}^z a_j(t) \varphi_j(\mathbf{r})$, where

$\varphi_j(\mathbf{r})$ is the reduced basis obtained using the POD technique [4] on a given ensemble of ODF information. More details on how this basis is defined, generated and its advantages over a full model can be obtained from [3, 4]. Several interesting design examples are documented in [3], which highlight the effectiveness of the proposed methodology towards microstructure sensitive design of deformation processes. As an example, we briefly summarize the problem involving the design of the velocity gradient (at a material point, homogeneous problem) for a required distribution of the Lankford parameter about the rolling direction. The desired distribution of the R-parameter is shown in Fig. 4, along with the various distributions obtained at different stages of optimization. Also shown is the ODF represented over the fundamental region using the full model and the reduced modeling schemes. A coupled macro–micro analysis is employed to develop continuous expressions for the angular distribution of the Lankford coefficient for the R value based on Hill’s anisotropic yield criterion. The design parameter, the velocity gradient L , is expressed as linear combination of 5 different deformation modes: 1 uniaxial tension, 1 plane strain compression and 3 simple shears (and represented by the 5 coefficients as α which quantifies the magnitude of each mode [4]). The desired $\alpha = \{1.2, 0, 0, 0, 0\}$, while the optimum α was obtained as $\{1.19, 0.047, 0.001, 0.005, 0\}$, which is a very good estimation of the desired velocity gradient. To the best of our knowledge this is the first time optimizing microstructure dependent properties has been mathematically addressed and a solution process developed.

1.5 Multi-length scale thermo -elasto-viscoplastic analysis [5]

The previous section described the framework for defining a design problem across length-scales. The main drawback with the analysis (in Section 1.4) was that elastic and thermal effects were neglected. Work is currently in progress to extend [3, 4] towards a truly multi-length scale design framework. This theory has been motivated based on the thermal activation theory for plastic flow. The kinematics of the problem is described in Fig. 5. In an appropriate

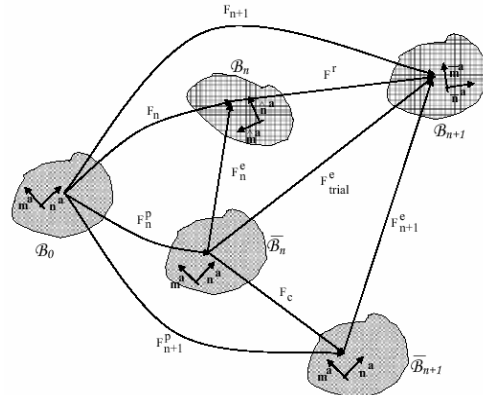


Fig. 5 Evolution of various material configurations for a single crystal as needed in the integration of the constitutive model - m denotes the slip direction and n the slip normal.

kinematic framework for large deformations, the total deformation gradient is decomposed into plastic and elastic parts as follows $F = F^e F^p$, where F^e is the elastic deformation gradient and F^p is the plastic deformation gradient. The evolution of the plastic flow is given by $\dot{F}^p F^{p-1} = \sum_j \dot{\gamma}^j S_0^j$, where $\dot{\gamma}^j$ is the shearing

rate and S_0^j is the Schmid tensor. In the constitutive framework defined for single crystals, Green elastic strain measures,

$$\bar{E}^e = \frac{1}{2}(F^{eT} F^e - I),$$

defined on the relaxed configuration, obtained by elastically unloading the current configuration and the corresponding

conjugate stress measure defined as $\bar{T} = \det F^e (F^{e-1} T F^{e-T})$, where T is the crystal Cauchy stress.

Further, the conjugate stress is defined as $\bar{T} = L^e [\bar{E}^e - A(\theta - \theta_0)]$, where A is the anisotropic thermal expansion tensor and L^e is the elasticity tensor. It is also common to consider obstacles to the motion of dislocations overcome with and without the aid of thermal fluctuations as thermal and athermal, respectively. Further, the shearing rate is also expressed in terms of the temperature and the activation energy of the average obstacle. Once, the single crystal response has been evaluated, the polycrystal response is computed through a linking hypothesis, here the Taylor hypothesis. Based on this hypothesis, the average of a field can be computed as $\langle \Theta \rangle = \int_{\Omega} \Theta(s, t) \hat{A}(s, 0) dV$, where

$\hat{A}(s, 0)$ is the initial ODF, which is assumed known. The equilibrium equation can be expressed on the reference configuration (here the total Lagrangian framework) based on a polycrystalline plasticity approach as, $\nabla_0 \cdot \langle P \rangle + f = 0$, where $\langle P \rangle$ is the averaged Piola Kirchhoff-1 stress. The weak form is evaluated and a Newton-Raphson approach is employed to solve the non-linear system of equations. The proposed modeling scheme is validated by comparison with experimental results available in literature. The experimental results of Carrekar and Hibbard [7] on 99.987 % pure polycrystalline f.c.c. Aluminum are used for this purpose. The material parameters are expressed in [5]. The experiments, simple shear tests, were performed at a constant strain rate of $6.667 \times 10^{-4} \text{ s}^{-1}$ and for temperatures varying from 20K to 300K. The predicted and experimental stress-strain responses are superposed in Fig 6. The material model is accurate for higher temperatures – and under-predicts at 20K. Preliminary investigation reveals that this under-prediction could be due to the result of a lower saturation value for the slip system resistances in the numerical experiments.

2 Personnel (partially supported)

N. Zabaraz (PI), S. Ganapathysubramanian, Velamur asokan Badri Narayanan, Swagato Acharjee (GRAs).

3 Interactions/Transitions

- Companies interacting with us include: General Electric (Srikanth Akkaram, a former PhD student from our group is now employed with GE-CRD), Pratt and Whitney (P&W) and Alcoa.
- Our collaboration with Alcoa is continuing towards the experimental evaluation of computational designs, on the design of flat-die extrusion and multiple-pass rolling processes as well as on the design of processes for damaged materials.
- The PI has reviewed this project in various agencies and universities including at AFOSR (5/29/02) [8], Rio de Janeiro, Brazil (8/16/02), NSF(1/6/03) [9], AFOSR (5/29/03), AFRL (7/21/03) & USNCCM (7/29/03).

References

[1] Deformation process design for control of microstructure in the presence of dynamic recrystallization and grain growth mechanisms, (with S. Ganapathysubramanian), Int. J. Solids

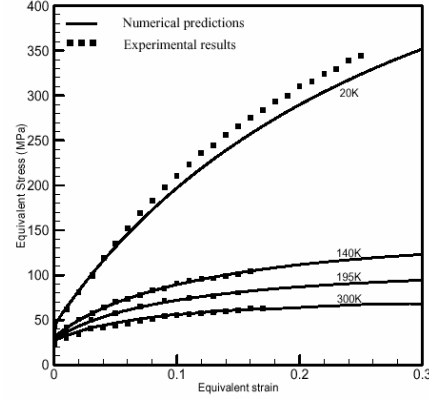


Fig. 6 Material response during a simple shear test of f.c.c. Aluminum [5].

Structures, in press.

[2] The continuum sensitivity method for the computational design of three-dimensional deformation processes, (with S. Acharjee), *Comp. Meth. Appl. Mech. Eng.*, submitted.

[3] Design across length scales: A reduced-order model of polycrystal plasticity for the control of microstructure-sensitive material properties, (with S. Ganapathysubramanian), *Comp. Meth. Appl. Mech. Eng.*, submitted.

[4] A proper orthogonal decomposition approach to microstructure model reduction in Rodrigues space with applications to the control of material properties, (with S. Acharjee), *Acta Materialia*, Vol. 51/18, pp. 5627-5646, 2003.

[5] Modeling the thermoelastic-viscoplastic response of polycrystals using a continuum representation over the orientation space, (with S. Ganapathysubramanian), *Int. J. Plasticity*, submitted.

[6] A continuum sensitivity method for the design of multi-stage metal forming processes, (with S. Ganapathysubramanian and Q. Li), *Int. J. Mech. Sciences*, Vol. 45, pp. 325-358, 2003.

[7] Tensile deformation of aluminum as a function of temperature, strain rate and grain size, *Trans. AIME* 209, 1157-1163, 1957.

[8] Advanced computational techniques for the design of deformation processes, in the proceedings of the AFOSR Computational and Applied Mathematics Program Review, Ft Walton Beach, Florida, May 29-31, 2002.

[9] Development of a robust computational design simulator for industrial deformation processes, in the proceedings of the 2003 NSF Design, Service and Manufacturing Grantees Conference, Birmingham, Alabama, January 6-9, 2003.

[10] A continuum theory for dynamic recrystallization with microstructure related length scales, *Int. J. Plasticity* 14(4-5), 319-351, 1998.